Communication

In-Situ Monitoring Apoptosis Process by A Self-Reporting Photosensitizer

Tianfu Zhang, Yuanyuan Li, Zheng Zheng, Ruquan Ye, Yiru Zhang, Ryan T. K. Kwok, Jacky W. Y. Lam, and Ben Zhong Tang

J. Am. Chem. Soc., **Just Accepted Manuscript** • DOI: 10.1021/jacs.9b00636 • Publication Date (Web): 28 Mar 2019

In-Situ Monitoring Apoptosis Process by A Self-Reporting Photosensitizer

Tianfu Zhang,[†,§] Yuanyuan Li,[†,§] Zheng Zheng,[†] Ruquan Ye,[‖] Yiru Zhang,[‡] Ryan T. K. Kwok,[†] Jacky W. Y. Lam,[†] and Ben Zhong Tang,*[,†,‡]

[†] Department of Chemistry, Hong Kong Branch of Chinese National Engineering Research Center for Tissue Restoration and Reconstruction, Institute for Advanced Study, Institute of Molecular Functional Materials, Division of Life Science and State Key Laboratory of Molecular Neuroscience, Department of Chemical and Biological Engineering, The Hong Kong University of Science and Technology, Clear Water Bay, Kowloon, Hong Kong, China

[‡] Center for Aggregation-Induced Emission, State Key Laboratory of Luminescent Materials and Devices, SCUT-HKUST Joint Research Institute, South China University of Technology, Guangzhou 510640, China

[‖] Department of Chemistry, City University of Hong Kong, Hong Kong, China

Supporting Information Placeholder

ABSTRACT: Although photodynamic therapy (PDT) thrived as a promising treatment, highly active photosensitizers (PSs) and intense light power can cause treatment overdose. However, extra therapeutic response probes always make the monitoring process complicated, ex-situ and delayed. Now this challenge is addressed by a self-reporting cationic PS, named TPE-4EP+, with aggregation-induced emission characteristic. The molecule undergoes mitochondria-to-nucleus translocation during apoptosis induced by PDT, thus enabling the in-situ real-time monitoring via fluorescence migration. Moreover, by molecular charge engineering, we prove that the in-situ translocation of TPE-4EP+ is mainly attributed to the enhanced interaction with DNA imposed by its multi-valent positive charge. The ability of PS to provide PDT with real-time diagnosis help control the treatment dose that can avoid excessive phototoxicity and minimize potential side effect. Future development of new generation of PS is envisioned.

Cancers, especially malignant and cancerous ones, have become the leading causes of death worldwide.[1] The most common traditional cancer treatments, such as chemotherapy[2] and radiation therapy,[3] are adopted with a "to be safe" overdose strategy to ensure the complete removal of cancer cells and better therapeutic effect. However, drug overdose and excessive radiation always induce side effect and lesion of normal tissues. Even worse, it can increase the risk of developing cancer resistance and second cancers, and aggravate the situation.[4,5] Therefore, it is highly desirable to timely monitor the therapeutic responses in situ and to develop a more effective and noninvasive treatment method to avoid excessive damage.

Photodynamic therapy (PDT) emerges as a promising treatment modality thanks to its selective cytotoxicity towards cancer cells with high spatiotemporal precision and noninvasive nature.[6–8] The principle of PDT is that a photosensitizer (PS) is activated under light irradiation to generate toxic reactive oxygen species (ROS) such as singlet oxygen ($^1O_2$) to kill cancer cells.[9–11] Unfortunately, PDT shows also some drawbacks. For example, highly active PS and high power light can destroy normal cells and compromise therapeutic efficacy.[12,13] Hence, how to monitor PS work in the body and how to evaluate the exact treatment end point are important.

It is generally recognized that apoptosis can be induced by PDT. Thus, apoptosis sensing can provide valuable diagnosis information on the therapeutic efficacy.[14,15] The most common approach is monitoring the phosphatidylserine in early apoptotic cells by fluorescent dye-labeled annexin V coupled with nuclear stains, usually combining with flow cytometry.[16,17] Although this technique provides quantitative data, its temperature sensitivity, extracellular Ca^{2+} concentration and operational demanding make it impractical for in-situ and real-time monitoring of the apoptosis process. To address this problem, fluorescent probes with aggregation-induced emission (AIE) characteristics[18] were first developed by Tang[19] for real-time drug evaluation and apoptosis monitoring.[20–22] On the other hand, Hong et. al reported a positively charged AIE luminogen (AIEgen) for nucleus staining in dead cell due to its entry to the fragmented nucleus and bound to DNA electrostatically.[23] Although nonemissive in solution state, emission of AIEgen is activated by interacting with DNA due to the restriction of intramolecular rotations (RIR) to reduce the nonradiative decay.[24–26] However, all the reported probes serve only as the drug reporter and extra PSs are needed in the therapeutic process. To the best of our knowledge, highly efficient PSs enabling real-time and in situ evaluation of its therapeutic effect remain challenging. In most biological systems, some apoptosis inducing factors will undergo translocation from mitochondria to the nucleus during apoptosis,[27,28] accompanying with mitochondrial depolarization,[29] membrane permeabilization and DNA fragementation.[15] Imitating this intelligent biological process, we worked on the design of new AIEgens for PDT monitoring system. The new molecule called TPE-4EP+ exhibits extremely high $^1O_2$ generation efficiency. In addition, it undergoes mitochondria-to-nucleus translocation during apoptosis induced by PDT, enabling the construction of a real-time self-reporting system to monitor the PDT process in situ. In comparison, through adjusting the electrostatic interaction between molecules and DNA, double and triple positively charged AIEgens possess

PDT effect, but no clear translocation signal and apoptosis monitoring ability were synthesized as control. With diagnostic information provided from the self-reporting photodynamic therapy system, fine control on the treatment time is possible to avoid phototoxicity overdose and reduce potential side effect.

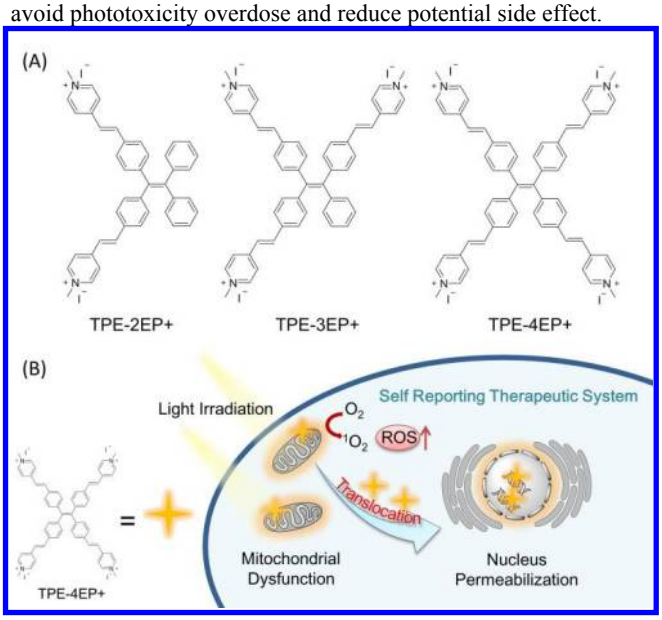

Figure 1. (A) Molecular structures of TPE-2EP+, TPE-3EP+ and TPE-4EP+. (B) Proposed Mechanism of mitochondria-to-nucleus translocation of TPE-4EP+.

To investigate the charge effect, we synthesized a series of fluorogens: TPE-2EP+, TPE-3EP+ and TPE-4EP+ by adjusting the number of pyridinium moiety (Figure 1A).[30] Their chemical structures and optical properties were characterized and summarized (Scheme S1–S2, Figure S1–S5, Table S1). Because of their ionic character, all the molecules exhibited good water-solubility and weak emission. After increasing the fraction of EtOH as the poor solvent, the emission intensities gradually increased (Φ = 15%, peak emission = 610 nm) due to RIR when aggregate formation. Clearly, three molecules possess AIE characteristics.

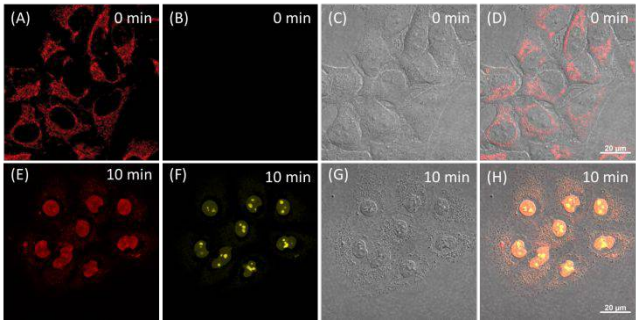

Figure 2. Confocal imaging of HeLa Cells (A−D) before (0 min, upper panel) and (E−H) after white light irradiation for 10 min (lower panel) stained with (A,E) TPE-4EP+, (B,F) PI and (C,G) Bright-field. (D, H) Merged images of Panel (A) and (B), (E) and (F).

The unique emission enhancement phenomenon, good water-solubility and intense long-wavelength emission of these molecules encouraged us to investigate its bioapplication.[31,32] Figure S6 illustrated the colocalization image of stained cell. Clearly, the mitochondria can be visualized with bright fluorescence and showed high specificity (Figure S7). Their mitochondria-targeting behavior could be attributed to electrostatic interaction between negative transmembrane potential of mitochondria within cancer cell and positively charged pyridinium moiety, which restricts the intramolecular rotation of molecules and boosts emission.[33–35] In contrast, the normal-cell-staining experiments exhibited negligible fluorescence, which suggests the molecules have extraordinary selectivity for cancer cells staining (Figure S8-S9). Correlate experiments were also provided that selective accumulation of TPE-4EP+ in cancer cells is due to the higher mitochondria membrane potential of cancer cells over normal cells (Figure S10–S11).[36]

Surprisingly, when we subsequently evaluated the photostability of three molecules by continuous laser excitation, only TPE-4EP+ was observed to redistribute from mitochondrial to nucleus gradually (Figure S12–S16). We further investigated the phenomenon by performing cell imaging of TPE-4EP+ with white light exposure. Originally, TPE-4EP+ stained the mitochondria exclusively (Figure 2). However, after 10 min of white light illumination, TPE-4EP+ mainly redistributed in nucleus while the area of mitochondrial seemed fragmented and showed negligible fluorescent signal. Furthermore, cell shrinkage, membrane blebbing and morphology change can be visualized in the bright field images, which are the traits of cell apoptosis.

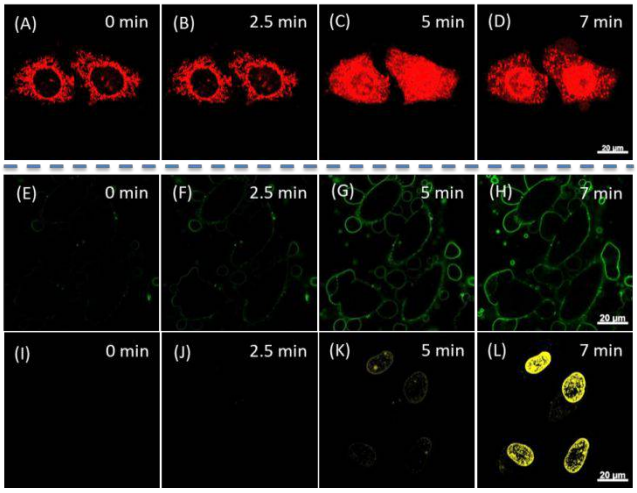

Figure 3. Real-time confocal imaging of HeLa Cells under continuous 405 laser irradiation stained with (A−D) TPE-4EP+ (upper panel). Real-time confocal imaging of HeLa Cells under the same condition stained with TPE-4EP+, followed by the addition of (E−H) Annexin V-FITC and (I−L) PI.

Aiming to testify the mechanism of fluorescence translocation phenomenon, FITC-annexin V and propidium iodide (PI) assay is used to identify early and late stage apoptotic versus necrosis. The real-time imaging of TPE-4EP+ was performed (Video S1). Briefly, HeLa cells were treated with TPE-4EP+ as the PS and subsequently stained with annexin V and PI, followed by light exposing to induce cell death. As shown in Figure 3, TPE-4EP+ anchored to mitochondria of the healthy cells at the beginning. After continuous 5-minutes laser irradiation, fluorescent signal from FITC emerged surrounding the cell membrane while PI signal was still invisible. As annexin V is able to stain early-stage apoptotic cells while PI only stains dead cells or late-stage apoptotic cells, the result of 5-minute laser irradiation indicates that the cells were at the early stage of apoptosis.[37] With continuous irradiation, the integrity of the cell membranes was destroyed and the PI signal became obvious. It is worth noting that TPE-4EP+ underwent fluorescence translocation from mitochondria to nucleus gradually and the signal mainly located in nucleus at final point. Meanwhile, cell apoptosis under light

irradiation was confirmed by annexin V-FITC/PI staining through flow cytometry (Figure S17), which was in agreement with that of cell-imaging experiments. Collectively, these evidences indicated that mitochondria-to-nucleus translocation of TPE-4EP+ was induced by cell apoptosis, which is the primary cause of effective therapeutic process. More importantly, the different stage of apoptosis could be differentiated clearly using TPE-4EP+.

Positively charged pyridinium salt in molecules has been reported to be an important functional group processing efficient PDT effect.[31,35] Therefore, the phenomenon of apoptosis process under light irradiation prompted us to investigate the phototoxicities of the molecules. First, the extracellular experiment was conducted by evaluating the efficiency of $^1O_2$ generation preliminarily, which plays a key role in PDT.[38,39] Under 80s of light irradiation, over 80% of 9,10-anthracenediylbis(methylene)dimalonic acid (ABDA), a commercially available $^1O_2$ indicator , was consumed at the presence of TPE-4EP+ in water solution. This approximated to a decomposition rate of 118.5 nmol min^{-1}, while that of TPE-2EP+ and TPE-3EP+ was 48.1 and 69.5 nmol min^{-1}, respectively (Figure S18). All the molecules are more effective than the commercial photosensitizer Rose Bengal (16.7 mmol min^{-1}). Then, we further studied the PDT effect of molecules as PSs by quantitatively evaluation on HeLa cells through MTT assay. Under white-light irradiation, three molecules exhibited superior phototoxicity (Figure S19). Meanwhile, the bright-green emission of dichlorofluorescein diacetate (DCFDA, a reactive oxygen species indicator) from cell incubation experiments also verified the $^1O_2$ production (Figure S20). Remarkably, the molecules exhibited high cell viability in dark condition. Low cytotoxicity towards HLF cells was also observed, suggesting their biocompatibility (Figure S21). Based on the results, $^1O_2$ generation efficiency is directly correlated with the charge numbers of molecules, in the sequence of TPE-2EP+ < TPE-3EP+ < TPE-4EP+. Collectively, without other extra agents, real-time in situ monitoring of apoptosis during PDT is afforded by simply visualizing the translocation phenomenon of TPE-4EP+ in cells, making it a self-reporting photodynamic theranostic system.

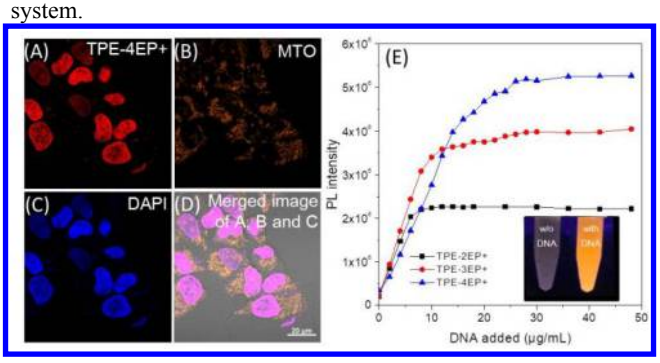

Figure 4. Confocal images of Fixed HeLa cells stained with 1 μM of (A)TPE-4EP+, 200 nM of (B) MTO and 1 μM of (C) DAPI. (D) Merged images of panels (A), (B) and (C). (E) The Plot of elevated PL intensity at 605 nm versus the ctDNA. Inset: photographs of TPE-4EP+ in water solution in the absence and presence of ctDNA taken under 365 nm UV irradiation.

To decipher the rationale behind the translocation of TPE-4EP+ during PDT treatment, 4% paraformaldehyde-fixed HeLa cells were treated with three molecules. The result showed that TPE-2EP+ can still stained the mitochondria of fixed cell while TPE-3EP+ spread throughout the whole cells and lost the specificity (Figure S22–S23). However, for the cell imaging of TPE-4EP+, only nucleus showed fluorescence and high specificity (Figure 4A–D). It is proposed that the different fluorescent performance during PDT treatment may be correlated with the specific interactions between molecules and some biomolecules in nucleus.

DNA, one of the most abundant components in nucleus, was reported previously to exhibit high affinity for cationic AIEgens by electrostatic force.[23,40,41] To testify the principle of the nucleus-targeting, we used calf thymus DNA (ctDNA) as a model (Figure 4E, Figure S24). Three molecules exhibited the PL enhancing effect after adding ctDNA in the order of TPE-2EP+ < TPE-3EP+ < TPE-4EP+, which was in accordance with the sequence of increasing numbers of charge carried. This interesting result indicates that the molecules with more positively charged pyridinium moieties on their branch could dock on the surfaces and in the cavities of the negatively charged DNA via electrostatic interactions. The intramolecular motions of phenyl rings are thus restricted to hinder nonradiative decay and strong emission is activated.[40]

Based on the above studies, we proposed the mechanism of mitochondria-to-nucleus translocation of TPE-4EP+ induced by $^1O_2$ generation upon PDT treatment (Figure 1B). At the beginning, TPE-4EP+ stains mitochondria specifically due to its high affinity to negatively charged mitochondrial membrane. After laser or white light irradiation, photosensitized $^1O_2$ generates and induces the cell apoptosis, which involves the depolarization of the mitochondrial membrane potential, increase of cell permeability, and degradation of nuclear DNA. Therefore, TPE-4EP+ could detach and lose its targeting ability after mitochondrial dysfunction during cell death by photodynamic effect, subsequently relocate and illumine the nucleus by binding to the nuclear DNA strongly through electrostatic interaction.

In summary, TPE-4EP+ can not only induce cell apoptosis by the intrinsic high $^1O_2$ generation efficiency under irradiation, but also clearly differentiate health and apoptotic cells without any additional agents. Since TPE-4EP+ specifically stains HeLa cancer cells, cytotoxicity to normal cells can be mitigated. Particularly, the fluorescent PS can serve as a self-reporter to monitor the PDT process, such as where the cancer cell locates, how the PDT performs, and when is the end point of PDT. Our work opens a new way for visualizing the photodynamic therapy so that the control the phototoxicity dose is possible. In addition, the working principle of TPE-4EP can provide strategy for the rational design of new generation of PS.

ASSOCIATED CONTENT

Supporting Information

The Supporting Information is available free of charge on the ACS Publications website.
Detailed methods, characterizations and supplementary figures (PDF)
Movie of real-time dynamic change of TPE-4EP+ (avi.)

AUTHOR INFORMATION

Corresponding Author

*tangbenz@ust.hk

Author Contributions

§T.Z. and Y.L. contributed equally to this work.

Notes

The authors declare the following competing financial interest(s): T.Z., Y.L., Z.Z. and B.Z.T. are the inventors of a patent filed by Hong Kong University of Science and Technology.

ACKNOWLEDGMENT

This work was financially supported by the National Science Foundation of China (21788102), the Research Grants Council of Hong Kong (16305518, C6009-17G and A-HKUST605/16), the Innovation and Technology Commission (ITC-CNERC14SC01 and ITS/254/17), the National Key Research and Development program of China (2018YFE0190200) and the Science and Technology Plan of Shen-zhen (JCYJ20160229205601482 and JCYJ20170818113602462).

REFERENCES

(1) Siegel, R. L.; Miller, K. D.; Jemal, A. Cancer Statistics, 2017. *CA. Cancer J. Clin.* **2017**, *67* (1), 7–30.

(2) Chabner, B. A.; Roberts Jr, T. G. Chemotherapy and the War on Cancer. *Nat. Rev. Cancer* **2005**, *5*, 65.

(3) Fan, W.; Shen, B.; Bu, W.; Chen, F.; Zhao, K.; Zhang, S.; Zhou, L.; Peng, W.; Xiao, Q.; Xing, H.; et al. Rattle-Structured Multifunctional Nanotheranostics for Synergetic Chemo-/Radiotherapy and Simultaneous Magnetic/Luminescent Dual-Mode Imaging. *J. Am. Chem. Soc.* **2013**, *135* (17), 6494–6503.

(4) Gottesman, M. M.; Fojo, T.; Bates, S. E. Multidrug Resistance in Cancer: Role of ATP–dependent Transporters. *Nat. Rev. Cancer* **2002**, *2*, 48.

(5) Holohan, C.; Van Schaeybroeck, S.; Longley, D. B.; Johnston, P. G. Cancer Drug Resistance: An Evolving Paradigm. *Nat. Rev. Cancer* **2013**, *13*, 714.

(6) Zhou, Z.; Song, J.; Nie, L.; Chen, X. Reactive Oxygen Species Generating Systems Meeting Challenges of Photodynamic Cancer Therapy. *Chem. Soc. Rev.* **2016**, *45* (23), 6597–6626.

(7) Liu, S.; Zhang, H.; Li, Y.; Liu, J.; Du, L.; Chen, M.; Kwok, R. T. K.; Lam, J. W. Y.; Phillips, D. L.; Tang, B. Z. Strategies to Enhance the Photosensitization: Polymerization and the Donor–Acceptor Even–Odd Effect. *Angew. Chemie Int. Ed.* **2018**, *57* (46), 15189–15193.

(8) Gottesman, M. M.; Fojo, T.; Bates, S. E. Multidrug Resistance in Cancer: Role of ATP–dependent Transporters. *Nat. Rev. Cancer* **2002**, *2*, 48.

(9) Guo, L.; Niu, G.; Zheng, X.; Ge, J.; Liu, W.; Jia, Q.; Zhang, P.; Zhang, H.; Wang, P. Single Near-Infrared Emissive Polymer Nanoparticles as Versatile Phototheranostics. *Adv. Sci.* **2017**, *4* (10), 1700085.

(10) Zheng, X.; Ge, J.; Wu, J.; Liu, W.; Guo, L.; Jia, Q.; Ding, Y.; Zhang, H.; Wang, P. Biodegradable Hypocrellin Derivative Nanovesicle as a Near-Infrared Light-Driven Theranostic for Dually Photoactive Cancer Imaging and Therapy. *Biomaterials* **2018**, *185*, 133–141.

(11) Celli, J. P.; Spring, B. Q.; Rizvi, I.; Evans, C. L.; Samkoe, K. S.; Verma, S.; Pogue, B. W.; Hasan, T. Imaging and Photodynamic Therapy: Mechanisms, Monitoring, and Optimization. *Chem. Rev.* **2010**, *110* (5), 2795–2838.

(12) Sharma, B. R. Infection in Patients with Severe Burns: Causes and Prevention Thereof. *Infect. Dis. Clin. North Am.* **2007**, *21* (3), 745–759.

(13) Lapotko, D. O.; Zharov, V. P. Spectral Evaluation of Laser-Induced Cell Damage With Photothermal Microscopy. **2005**, *36* (1), 22–30.

(14) Andón, F. T.; Fadeel, B. Programmed Cell Death: Molecular Mechanisms and Implications for Safety Assessment of Nanomaterials. *Acc. Chem. Res.* **2013**, *46* (3), 733–742.

(15) Nagata, S. Apoptosis and Clearance of Apoptotic Cells. *Annu. Rev. Immunol.* **2018**, *36* (1), 489–517.

(16) Zheng, H.; Wang, F.; Wang, Q.; Gao, J. Cofactor-Free Detection of Phosphatidylserine with Cyclic Peptides Mimicking Lactadherin. *J. Am. Chem. Soc.* **2011**, *133* (39), 15280–15283.

(17) Perfetto, S. P.; Chattopadhyay, P. K.; Roederer, M. Seventeen-Colour Flow Cytometry: Unravelling the Immune System. *Nat. Rev. Immunol.* **2004**, *4* (8), 648–655.

(18) Mei, J.; Leung, N. L. C.; Kwok, R. T. K.; Lam, J. W. Y.; Tang, B. Z. Aggregation-Induced Emission: Together We Shine, United We Soar! *Chem. Rev.* **2015**, *115* (21), 11718–11940.

(19) Luo, J.; Xie, Z.; Lam, J. W. Y.; Cheng, L.; Chen, H.; Qiu, C.; Kwok, H. S.; Zhan, X.; Liu, Y.; Zhu, D.; et al. Aggregation-Induced Emission of 1-Methyl-1,2,3,4,5-Pentaphenylsilole. *Chem. Commun.* **2001**, *18* (0), 1740–1741.

(20) Leung, A. C. S.; Zhao, E.; Kwok, R. T. K.; Lam, J. W. Y.; Leung, C. W. T.; Deng, H.; Tang, B. Z. An AIE-Based Bioprobe for Differentiating the Early and Late Stages of Apoptosis Mediated by H_2O_2. *J. Mater. Chem. B* **2016**, *4* (33), 5510–5514.

(21) Yuan, Y.; Kwok, R. T. K.; Tang, B. Z.; Liu, B. Targeted Theranostic Platinum(IV) Prodrug with a Built-In Aggregation-Induced Emission Light-Up Apoptosis Sensor for Noninvasive Early Evaluation of Its Therapeutic Responses in Situ. *J. Am. Chem. Soc.* **2014**, *136* (6), 2546–2554.

(22) Shi, H.; Kwok, R. T. K.; Liu, J.; Xing, B.; Tang, B. Z.; Liu, B. Real-Time Monitoring of Cell Apoptosis and Drug Screening Using Fluorescent Light-Up Probe with Aggregation-Induced Emission Characteristics. *J. Am. Chem. Soc.* **2012**, *134* (43), 17972–17981.

(23) Hong, Y.; Chen, S.; Leung, C. W. T.; Lam, J. W. Y.; Tang, B. Z. Water-Soluble Tetraphenylethene Derivatives as Fluorescent “Light-up” Probes for Nucleic Acid Detection and Their Applications in Cell Imaging. *Chem. - An Asian J.* **2013**, *8* (8), 1806–1812.

(24) Liu, S.; Cheng, Y.; Zhang, H.; Qiu, Z.; Kwok, R. T. K.; Lam, J. W. Y.; Tang, B. Z. In Situ monitoring of RAFT Polymerization by Tetraphenylethylene-Containing Agents with Aggregation-Induced Emission Characteristics. *Angew. Chemie Int. Ed.* **2018**, *57* (21), 6274–6278.

(25) Chen, J.; Law, C. C. W.; Lam, J. W. Y.; Dong, Y.; Lo, S. M. F.; Williams, I. D.; Zhu, D.; Tang, B. Z. Synthesis, Light Emission, Nanoaggregation, and Restricted Intramolecular Rotation of 1,1-Substituted 2,3,4,5-Tetraphenylsiloles. *Chem. Mater.* **2003**, *15* (7), 1535–1546.

(26) Shi, J.; Chang, N.; Li, C.; Mei, J.; Deng, C.; Luo, X.; Liu, Z.; Bo, Z.; Dong, Q. Y.; Tang, B. Z. Locking the phenyl rings of tetraphenylethene step by step: understanding the mechanism of aggregation-induced emission. *Chem. Commun.* **2012**, *48* (81), 10675–10677.

(27) Lorenzo, H. K.; Susin, S. A.; Penninger, J.; Kroemer, G. Apoptosis Inducing Factor (AIF): A Phylogenetically Old, Caspase-Independent Effector of Cell Death. *Cell Death Differ.* **1999**, *6*, 516.

(28) Daugas, E.; Susin, S. A.; Zamzami, N.; Ferri, K. F.; Irinopoulou, T.; Larochette, N.; Prevost, M.-C.; Leber, B.; Andrews, D.; Penninger, J.; et al. Mitochondrio-Nuclear Translocation of AIF in Apoptosis and Necrosis. *FASEB J.* **2000**, *14* (5), 729–739.

(29) Boren, J.; Brindle, K. M. Apoptosis-Induced Mitochondrial Dysfunction Causes Cytoplasmic Lipid Droplet Formation. *Cell Death Differ.* **2012**, *19* (9), 1561–1570.

(30) Wang, Z. Y.; Jiang, C.; Wu, J. H.; Guo, Q. X.; Yong, Z. A Novel Palladium-Catalyzed Reaction and Its Application in Preparation of Derivatives of Stilbazols. **2001**, *12* (5), 399–402.

(31) Zheng, Z.; Zhang, T.; Liu, H.; Chen, Y.; Kwok, R. T. K.; Ma, C.; Zhang, P.; Sung, H. H. Y.; Williams, I. D.; Lam, J. W. Y.; et al. Bright Near-Infrared Aggregation-Induced Emission Luminogens with Strong Two-Photon Absorption, Excellent Organelle Specificity, and Efficient Photodynamic Therapy Potential. *ACS Nano* **2018**, *12* (8), 8145–8159.

(32) Wang, Y.; Chen, M.; Alifu, N.; Li, S.; Qin, W.; Qin, A.; Tang, B. Z.; Qian, J. Aggregation-Induced Emission Luminogen with Deep-Red Emission for Through-Skull Three-Photon Fluorescence Imaging of Mouse. *ACS Nano* **2017**, *11* (10), 10452–10461.

(33) Leung, C. W. T.; Hong, Y.; Chen, S.; Zhao, E.; Lam, J. W. Y.; Tang, B. Z. A Photostable AIE Luminogen for Specific Mitochondrial Imaging and Tracking. *J. Am. Chem. Soc.* **2013**, *135* (1), 62–65.

(34) Chen, B.; Le, W.; Wang, Y.; Li, Z.; Wang, D.; Ren, L.; Lin, L.; Cui, S.; Hu, J. J.; Hu, Y.; et al. Targeting Negative Surface Charges of Cancer Cells by Multifunctional Nanoprobes. *Theranostics* **2016**, *6* (11), 1887–1898.

(35) Wang, D.; Lee, M. M. S.; Shan, G.; Kwok, R. T. K.; Lam, J. W. Y.; Su, H.; Cai, Y.; Tang, B. Z. Highly Efficient Photosensitizers with Far-Red/Near-Infrared Aggregation-Induced Emission for In Vitro and In Vivo Cancer Theranostics. *Adv. Mater.* **2018**, *30* (39), 1802105.

(36) Gui, C.; Zhao, E.; Kwok, R. T. K.; Leung, A. C. S.; Lam, J. W. Y.; Jiang, M.; Deng, H.; Cai, Y.; Zhang, W.; Su, H.; et al. AIE-Active Theranostic System: Selective Staining and Killing of Cancer Cells. *Chem. Sci.* **2017**, *8* (3), 1822–1830.

(37) Kumar, R.; Han, J.; Lim, H.-J.; Ren, W. X.; Lim, J.-Y.; Kim, J.-H.; Kim, J. S. Mitochondrial Induced and Self-Monitored Intrinsic Apoptosis by Antitumor Theranostic Prodrug: In Vivo Imaging and Precise Cancer Treatment. *J. Am. Chem. Soc.* **2014**, *136* (51), 17836–17843.

(38) Lan, M.; Guo, L.; Zhao, S.; Zhang, Z.; Jia, Q.; Yan, L.; Xia, J.; Zhang, H.; Wang, P.; Zhang, W. Carbon Dots as Multifunctional Phototheranostic Agents for Photoacoustic/Fluorescence Imaging and

Photothermal/Photodynamic Synergistic Cancer Therapy. *Adv. Ther.* **2018**, *1* (6), 1800077.

(39) Ge, J.; Lan, M.; Zhou, B.; Liu, W.; Guo, L.; Wang, H.; Jia, Q.; Niu, G.; Huang, X.; Zhou, H.; et al. A Graphene Quantum Dot Photodynamic Therapy Agent with High Singlet Oxygen Generation. *Nat. Commun.* **2014**, *5*, 4596.

(40) Wang, M.; Zhang, D.; Zhang, G.; Tang, Y.; Wang, S.; Zhu, D. Fluorescence Turn-On Detection of DNA and Label-Free Fluorescence Nuclease Assay Based on the Aggregation-Induced Emission of Silole. *Anal. Chem.* **2008**, *80* (16), 6443–6448.

(41) Yu, C. Y. Y.; Zhang, W.; Kwok, R. T. K.; Leung, C. W. T.; Lam, J. W. Y.; Tang, B. Z. A Photostable AIEgen for Nucleolus and Mitochondria Imaging with Organelle-Specific Emission. *J. Mater. Chem. B* **2016**, *4* (15), 2614–2619.

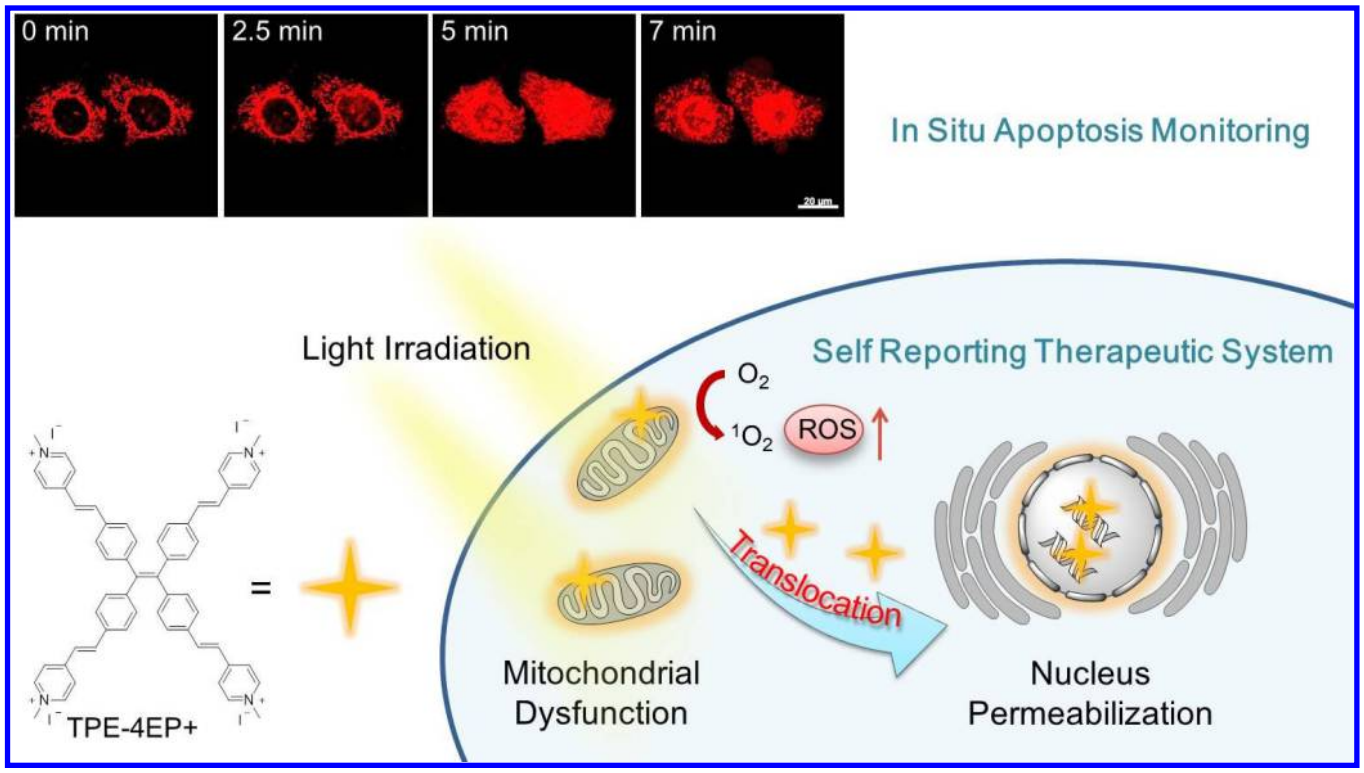
0 min
2.5 min
5 min
7 min
In Situ Apoptosis Monitoring
Light Irradiation
Self Reporting Therapeutic System
O_2
$^1O_2$
ROS
TPE-4EP+
=
Translocation
Mitochondrial Dysfunction
Nucleus Permeabilization